AUV Adaptive Yo-Yo Based on Layer Peak and Edge Detection and Its Application to Imaging Plankton Layers Using an Onboard Microscopy System

Yanwu Zhang, *Senior Member*, *IEEE*, Brian Kieft, *Member*, *IEEE*, Paul Roberts,
Brett W. Hobson, *Member*, *IEEE*, Quinn Shemet, *Member*, *IEEE*, and Thom Maughan

Abstract

In oceanographic surveys by autonomous underwater vehicles (AUVs), a routinely adopted survey pattern is a sawtooth (i.e., yo-yo) trajectory with pre-programmed depth bounds. In studies of oceanic layers, we desire the AUV survey to be concentrated in the high-signal layer, not wasting time at low-signal depths. In this paper, we present an adaptive yo-yo algorithm based on layer peak and edge detection. As the AUV traverses a layer, the measured signal level rises on the vehicle's entry into the layer and then falls on the vehicle's departure from the layer. When the signal level falls below a certain fraction of the peak level, the vehicle declares edge detection and flips attitude (i.e., turns from descent to ascent or conversely). Thus the vehicle transects the layer on an adaptive yo-yo trajectory that tracks the layer as its depth and thickness vary. This method was applied to plankton layer imaging by a long-range AUV (LRAUV) equipped with an *in situ* microscopy system. In an April 2025 experiment, the LRAUV tracked and imaged plankton layers on an adaptive yo-yo transect along Monterey Canyon.

Index Terms

Adaptive yo-yo, plankton layer, long-range autonomous underwater vehicle (LRAUV), microscopy

Corresponding author: Yanwu Zhang. Yanwu Zhang, Brian Kieft, Paul Roberts, Brett W. Hobson, Quinn Shemet, and Thom Maughen are with the Monterey Bay Aquarium Research Institute (MBARI), 7700 Sandholdt Road, Moss Landing, CA 95039, USA (e-mail: yzhang@mbari.org; bkieft@mbari.org; proberts@mbari.org; hobson@mbari.org; quinn@mbari.org; tm@mbari.org)

I. Introduction

In oceanographic surveys by autonomous underwater vehicles (AUVs), a routinely adopted survey pattern is a sawtooth (i.e., yo-yo) trajectory with pre-programmed depth bounds (or bottom-terminated when the seabed is detected) [1]–[3]. This survey pattern effectively depicts various water-column properties (temperature, salinity, etc.) on the transects. However, yo-yo surveys with fixed depth bounds may not be efficient for investigating oceanic layers since a large proportion of the survey time may be spent at depths with low levels of the signal of interest which in turn lowers the horizontal temporal and spatial resolution of the survey.

Physical and biological processes drive the formation of plankton aggregations in the horizontal and vertical dimensions [4]–[6]. Plankton layers are often observed in coastal and open oceans. They have an important impact on primary productivity, the development of harmful algal blooms (HABs), and other aspects of ocean ecology [7]–[9]. We previously developed methods for AUVs to autonomously find phytoplankton layers and acquire water samples at the signal peak in the layer [10]–[12].

At the Monterey Bay Aquarium Research Institute (MBARI), we developed *Tethys*-class long-range AUVs (LRAUVs) [13] that can carry an *in situ* microscopy system. This mobile microscope is tasked with imaging plankton layers. For efficient use of survey time and image recording storage, we desire the vehicle's yo-yo trajectory to be concentrated within the layer of high plankton signal levels. However, the layer's depth and thickness are unknown beforehand and vary in space and time. Therefore we need to enable the LRAUV to adaptively determine the yo-yo depth bounds on the fly.

AUVs were used to detect and track the thermocline layer on yo-yo trajectories with depth bounds adaptively defined based on the AUV-measured vertical temperature gradient [14]–[17]. We previously developed an adaptive yoyo-zigzag algorithm for an AUV to map patchy fields [18]. In the vertical dimension, the vehicle flies on a yo-yo trajectory (with preset depth bounds) and extracts the maximum signal value on each descent or ascent yo-yo profile, i.e., the per-yoyo maximum. In the horizontal dimension, the vehicle detects the peak and the edge of a patch, and accordingly determines when to turn onto the next zigzag leg.

In this paper, we present an adaptive yo-yo algorithm based on layer peak and edge detection. The LRAUV and the onboard microscopy system are introduced in Section II. The adaptive yo-yo algorithm is described in Section III. In April 2025, an LRAUV carrying the onboard microscope ran the algorithm to image plankton layers in Monterey Bay, California, as reported in Section IV. Conclusion and future work are discussed in Section V.

II. LRAUV WITH AN ONBOARD MICROSCOPY SYSTEM

Tethys-class LRAUVs were developed at the Monterey Bay Aquarium Research Institute (MBARI). Each vehicle is 2.3 m long (in basic configuration), and has a diameter of 0.3 m at the midsection (Figure 1). It can run from 0.5 m/s to 1.4 m/s using a propeller. Using a primary battery the vehicle has demonstrated a range of 1800 km (3-week duration) at 1 m/s speed [13]. Long range is realized by minimizing propulsion power consumption through an innovative design of a low-drag body, a high-efficiency propulsion system, and selective load control [13], [19]. In addition, the vehicle is equipped with a buoyancy engine and is capable of auto-ballasting to neutral buoyancy, which allows flight at a reduced angle of attack resulting in decreased drag. Using the buoyancy engine, the vehicle is capable of drifting in a lower power state and controlling depth while the thruster is powered off. An LRAUV thus combines mobility and speed properties typical of propelled vehicles and the energy saving properties unique to buoyancy-driven vehicles.

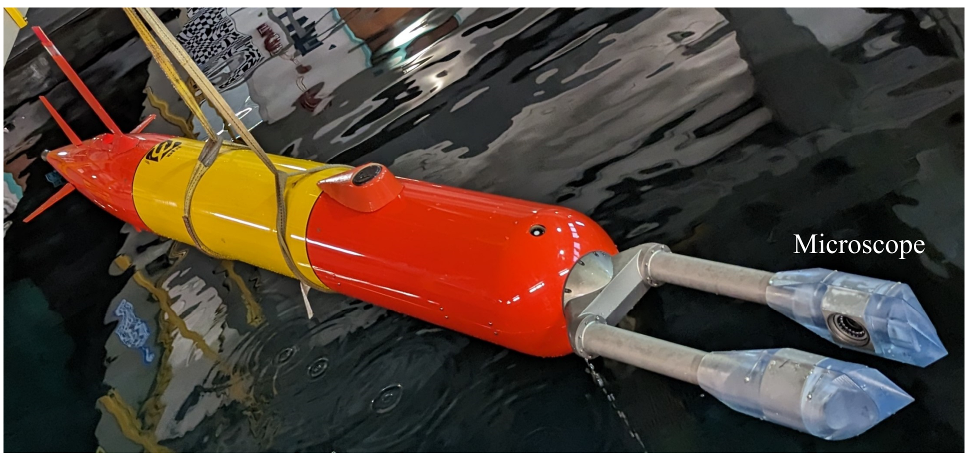

Fig. 1. A *Tethys*-class LRAUV equipped with a "Planktivore" microscopy system.

An LRAUV's standard science sensor suite includes Sea-Bird Glider Payload Conductivity-Temperature-Depth (GPCTD) sensors, a Sea-Bird SBE 43F dissolved oxygen sensor, a WET Labs ECO Triplet Puck fluorescence/backscatter sensor (chlorophyll fluorescence excitation wavelength 470 nm and emission wavelength 695 nm; backscatter of two wavelengths: 470 nm and 650 nm), and a LI-COR LI-192SA PAR (photosynthetically active radiation) sensor. The vehicle navigates underwater using dead reckoning aided by a Doppler Velocity Log (DVL). The DVL provides the Earth-referenced velocity of the vehicle when the ocean bottom is within acoustic range. The vehicle's estimated speed is combined with measured heading and attitude and then accumulated to provide the estimated location while underwater. The vehicle periodically ascends to the sea surface for global positioning system (GPS) fixes to correct the accumulated underwater navigation error [13].

The LRAUV software architecture uses state configured layered control [20], which divides the vehicle operation into a group of behaviors assigned with hierarchical levels of priority. The vehicle runs a mission script that invokes appropriate AUV behaviors to achieve a specified goal [13].

An *in situ* microscopy system (nicknamed “Planktivore”, developed at MBARI) can be installed at the nose of the LRAUV (Figure 1). The design of “Planktivore” was based on the Scripps Plankton Camera System [21] but adapted to work on autonomous vehicles. It uses two complementary microscope objectives (each with a camera and a light-emitting diode (LED) strobe) focused on a free-space volume in water roughly 12 mm away from each of the two viewports. This configuration enables free-space imaging of plankton, marine snow, and other suspended material that enter the sample volume via ambient flow. The imaging volume’s position outside of the vehicle bow wake helps to reduce avoidance. The microscopy system contains a pair of cameras. The high-magnification and low-magnification cameras cover particle size ranges from 20 μm to 200 μm, and from 100 μm to 2 cm, respectively. Onboard the imaging system, Regions of interest (ROIs) are detected in real time at a rate of 10 Hz for each magnification. The detection algorithm [21] uses traditional computer vision to find contours in the image, close the contours into foreground masks, and extract raw pixels from rectangular regions around each contour. The total number of detected contours is averaged over 10 frames and reported to the vehicle main computer in real time once per second, which provides an estimate of the *in situ* particle concentration.

III. Adaptive Yo-Yo Algorithm

The adaptive yo-yo algorithm is illustrated in Figure 2, and explained as follows. Suppose the signal layer deepens from west to east. When the AUV descends into the layer, the measured signal level rises and reaches the peak at point A. On the continued descent, the signal level falls. At point B, the signal level falls below a specified fraction (a parameter that defines the layer edge) of the peak level, causing the vehicle to declare edge detection. At this point, the vehicle flips from descent to ascent to re-enter the layer. The signal level rises on re-entry, reaches the peak at point C, and then falls on the continued ascent. At point D, the signal level falls below the specified fraction of the peak level, so the vehicle declares edge detection again. At this point, the vehicle flips from ascent to descent to re-enter the layer. Repeating this cycle, the AUV closely tracks and surveys the layer on an adaptive yo-yo trajectory.

To confine the yo-yo survey to depth ranges of interest, and for vehicle operational safety, we set shallow and deep limits for the yo-yo behavior. If the AUV reaches either limit before the signal has

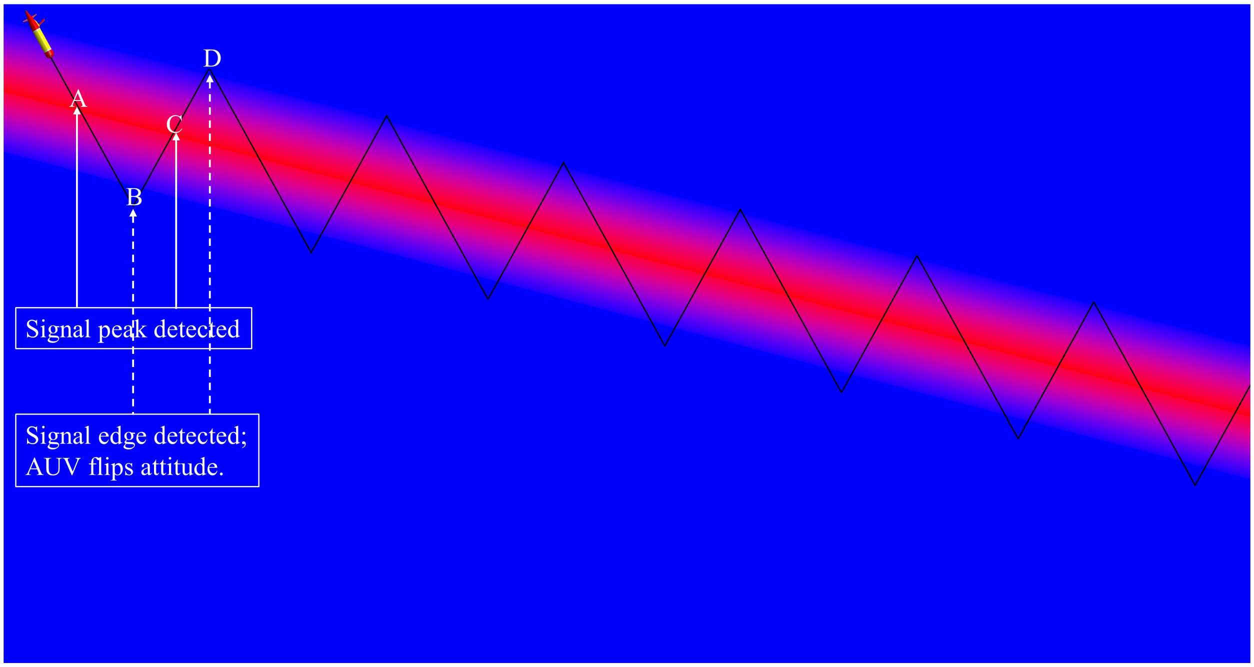

Fig. 2. Illustration of adaptive yo-yo through a layer based on signal peak and edge detection. Signal levels are indicated by the color spectrum from blue (low) to red (high).

fallen to the edge level, the vehicle nonetheless flips attitude.

IV. Field Experiment

In April 2025, LRAUV *Ahi* (carrying the "Planktivore" microscopy system) was deployed to image plankton layers along the Monterey Canyon. *Ahi* ran the adaptive yo-yo algorithm to achieve the goal of concentrating on layers of high particle concentration. The signal used was the frame-averaged counts of ROIs captured by Planktivore's low-magnification camera (i.e., the $\mathrm{ROI}_{\mathrm{LM}}$ signal). ROIs were detected at a frame rate of 10 Hz, then averaged over 10 frames and reported to the vehicle main computer once per second in real time. The low-magnification camera covers a size range from 100 μm to 2 cm which contains plankton and detritus [22], [23].

The edge signal level was defined as 50% of the peak level. As an example, Figure 3 shows signal peak and edge detection on an ascent profile. To suppress noise, the raw signal went through a 5-point median filter (for outlier rejection) followed by an 8-s moving-average window (for low-pass filtering). The signal reached the peak level at 63-m depth. At 54-m depth when the signal fell to 50% of the peak level, *Ahi* started to turn from ascent to descent (with a delay due to inertia).

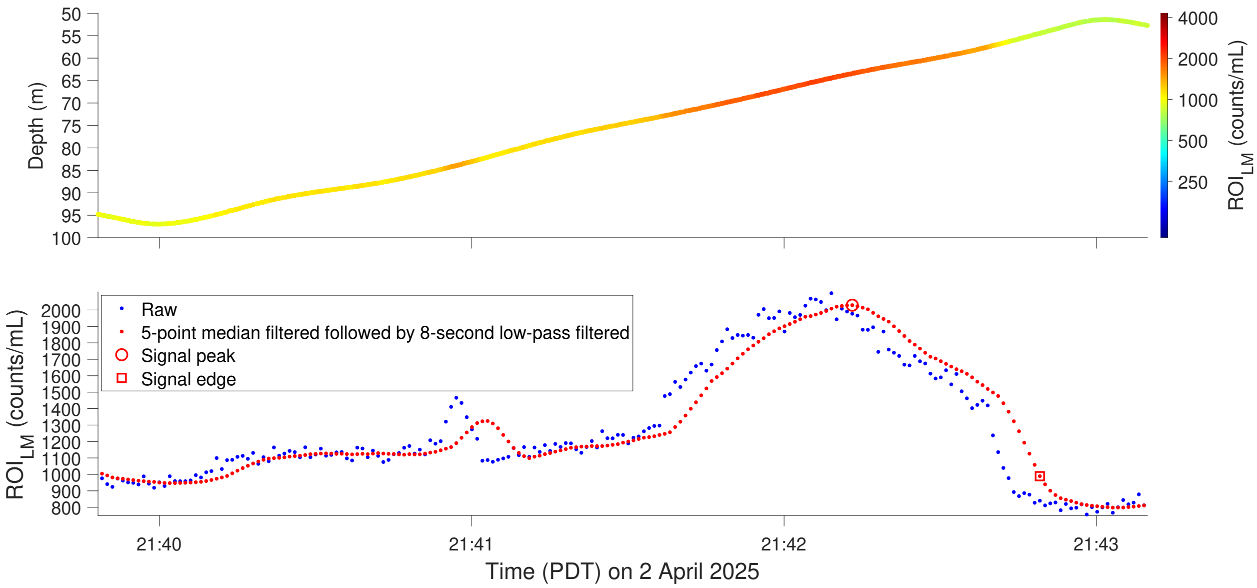

Fig. 3. LRAUV *Ahi*'s detection of signal peak and edge on one ascent profile out of a 10-hour adaptive yo-yo transect. The peak and the edge are marked by the circle and the square, respectively. The full 10-hour transect is plotted in Figure 4 and Figure 5.

Figure 4 shows *Ahi*-measured particle concentration signal on a 10-hour transect on an obtuse triangular loop along the canyon. The waypoints defining the programmed triangular track were: east vertex (36.797°N, 121.847°W), north vertex (36.803°N, 121.923°W), and west vertex (36.760°N, 121.970°W). *Ahi* started and ended at the east vertex. The vehicle ascended to the sea surface every hour for GPS fixes and transmission of decimated data to shore via Iridium satellite or cellular connection. *Ahi*'s speed through water was set to 1 m/s. However, a strong southward current kept deflecting the vehicle from the programmed track. Based on the discrepancies between the dead-reckoned locations (during submerged flight) and the GPS locations (attained at every surfacing), the vehicle fought hard to approach the desired waypoints. Consequently, *Ahi*'s horizontal speed over the ground dropped to about 0.6 m/s on the westbound segments (from the east vertex to the north vertex and then to the west vertex) and 0.7 m/s on the eastbound segment (from the west vertex to the east vertex). Its vertical speed on yo-yo profiles was about 0.25 m/s. *Ahi*'s actual track (lower panel of Figure 4) is based on the GPS fixes at the hourly surfacings, supplemented by two dead-reckoned locations at the west and east ends.

The 10-hour time series of the particle concentration signal is shown in Figure 5. On the entire transect, the yo-yo shallow limit was set to 2 m to keep the vehicle from breaching the sea surface. The north vertex of the programmed track was over the canyon's northern slope with shallower bathymetry. For

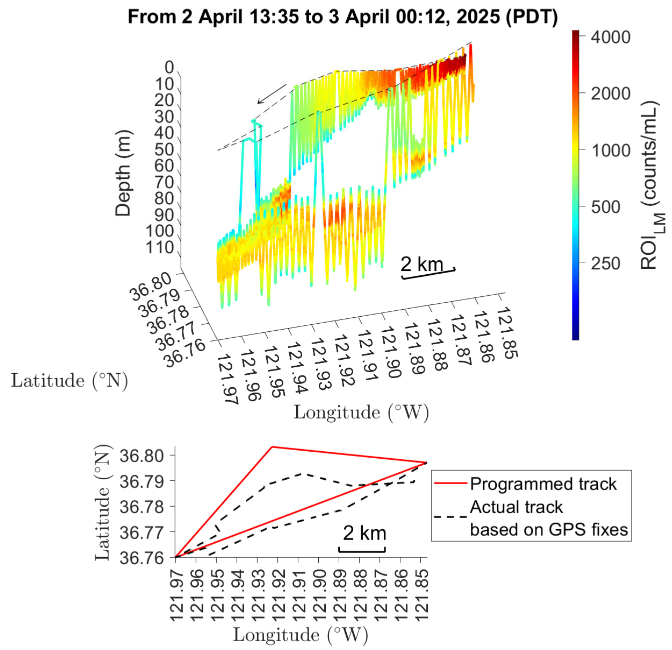

Fig. 4. Upper panel: perspective view of the particle concentration signal measured by *Ahi*'s onboard microscopy system on a 10-hour adaptive yo-yo transect (westward and then eastward) along Monterey Canyon. Lower panel: the programmed track compared with the actual track based on GPS fixes at hourly surfacings.

vehicle operational safety, the yo-yo deep limit was set to 80 m for the westward segments. The eastward segment was directly above the deep canyon, and the yo-yo deep limit was increased to 150 m.

From the start to 15:30, *Ahi* yo-yoed through a shallow plankton layer. From 15:30 to 17:20, the plankton layer deepened, thickened, and became less dense. From 17:20 to 19:23, *Ahi* detected a layer below 50-m depth. At the 80-m deep limit, the vehicle turned from descent to ascent even though the signal level was still higher than 50% of the peak level.

At 19:23 *Ahi* reached the west end and turned around onto the eastward segment. At this point the yo-yo deep limit switched from 80 m to 150 m. From 19:23 to 22:24, *Ahi* yo-yoed down to 100-m depth to cover the entire thickness of this deep layer, no longer clamped by the 80-m yo-yo deep limit. From 22:24 to the end, the plankton layer shoaled, with varying concentration and thickness.

Figure 6 shows a mosaic of images taken by the "Planktivore" microscopy system during the experiment which captured taxonomic diversity.

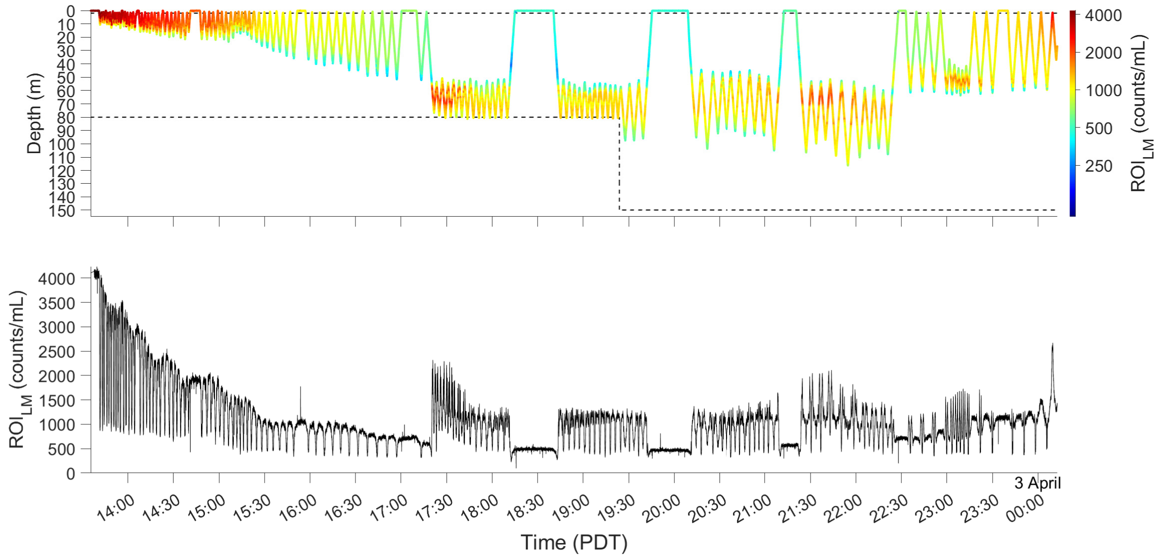

Fig. 5. Upper panel: time series of *Ahi*'s depth color-coded by the particle concentration signal. The shallow and deep limits of yo-yo are marked by the dashed lines. Lower panel: time series of the particle concentration signal.

V. Conclusion and Future Work

We developed an adaptive yo-yo algorithm based on layer peak and edge detection. An LRAUV carrying an *in situ* microscope ran the algorithm to image plankton layers along Monterey Canyon. The vehicle's yo-yo trajectory was concentrated within depths of high particle concentration as the layer depth and thickness varied along the transect.

After the April 2025 experiment, we have extended the algorithm as follows.

1) For layer edge detection, when we set the same off-peak fraction threshold (e.g., 50%) for ascent and descent legs, the yo-yo trajectory is centered at the layer peak, as in the unclamped segments shown in Figure 5. For carbon flux studies [24], we want the LRAUV-borne microscope to take images of the layer as well as the material sinking from the layer. To shift the yo-yo trajectory downward, we set different off-peak fraction thresholds for ascent and descent legs respectively, e.g., 75% for ascent legs and 25% for descent legs. On ascent, after passing the peak the vehicle turns to descent when the signal level is still high (75% of the peak level); on descent, the vehicle does not turn to ascent until the signal level is very low (25% of the peak level).
2) The LRAUV-borne microscopy system processes images onboard and reports taxonomic signal levels (e.g., diatoms and dinoflagellates) in real time. For targeted imaging of specific phytoplankton

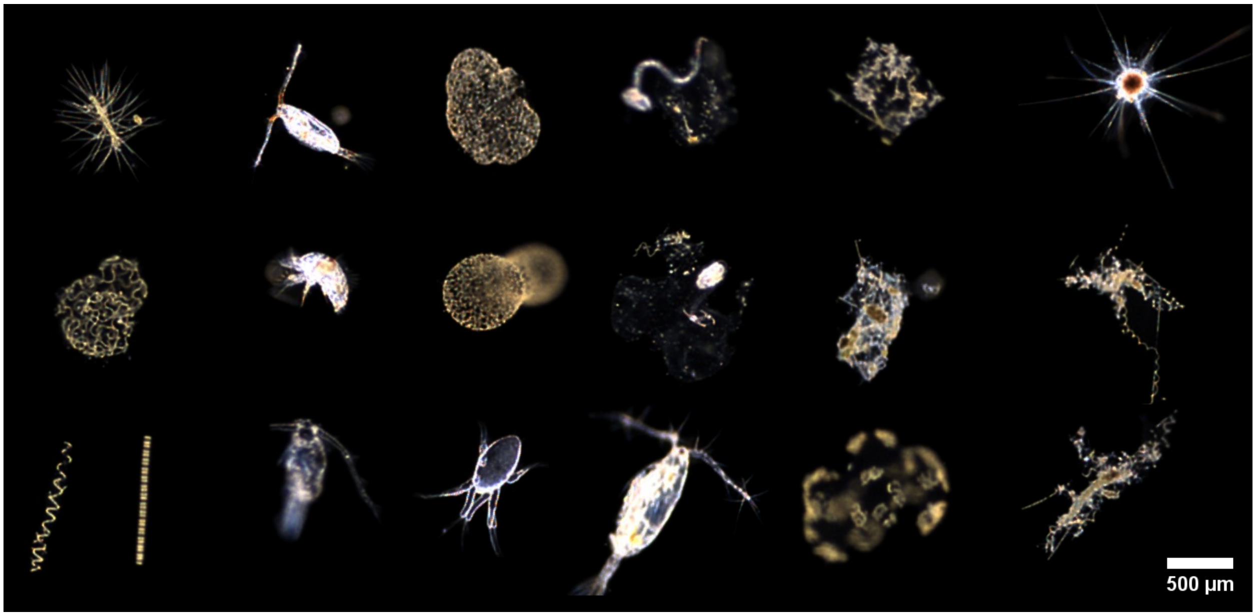

Fig. 6. Mosaic of images recorded by Planktivore's low-magnification camera during the experiment.

communities, the LRAUV uses the corresponding signal in peak and edge detection for determining the yo-yo depth bounds.

The expanded capacities will be tested in future experiments.

ACKNOWLEDGMENTS

This work was supported by the David and Lucile Packard Foundation. We thank Jon Erickson, Aaron Schnittger, Denis Klimov, and Irene Hu for contributions to the development and tests of the "Planktivore" microscopy system. We thank Varsha Senthil and Christopher Wahl for helping with the LRAUV operation, and Carlos Rueda for developing and supporting the LRAUV operation portal. We appreciate Colleen Durkin's comments and suggestions regarding carbon flux studies using mobile platforms.

REFERENCES

[1] X. Yu, T. Dickey, J. Bellingham, D. Manov, and K. Streitlien, "The application of autonomous underwater vehicles for interdisciplinary measurements in Massachusetts and Cape Cod Bays," *Continental Shelf Research*, vol. 22, pp. 2225–2245, 2002.

[2] M. A. Moline, S. M. Blackwell, C. von Alt, B. Allen, T. Austin, J. Case, N. Forrester, R. Goldsborough, M. Purcell, and R. Stokey, "Remote Environmental Monitoring Units: An autonomous vehicle for characterizing coastal environments," *Journal of Atmospheric and Oceanic Technology*, vol. 22, pp. 1797–1808, 2005.

[3] J. G. Bellingham, *Platforms: Autonomous Underwater Vehicles. In Encyclopedia of Ocean Sciences (J. H. Steele (ed.))*, 2nd ed. Waltham, MA: Academic Press, 2009.

[4] T. Sekino and N. Yamamura, "Diel vertical migration of zooplankton: optimum migrating schedule based on energy accumulation," *Evolutionary Ecology*, vol. 13, pp. 287–282, 1999.

[5] J. P. Ryan, M. A. McManus, J. D. Paduan, and F. P. Chavez, "Phytoplankton thin layers caused by shear in frontal zones of a coastal upwelling system," *Marine Ecology Progress Series*, vol. 354, pp. 21–34, 2008.

[6] J. P. Ryan, M. A. McManus, and J. M. Sullivan, "Interacting physical, chemical and biological forcing of phytoplankton thin-layer variability in Monterey Bay, California," *Continental Shelf Research*, vol. 30, no. 1, pp. 7–16, 2010.

[7] J. Huisman, N. Pham Thi, D. M. Karl, and B. Sommeijer, "Reduced mixing generates oscillations and chaos in the oceanic deep chlorophyll maximum," *Nature*, vol. 439, pp. 322–325, January 2006.

[8] M. A. McManus, R. M. Kudela, M. W. Silver, G. F. Steward, P. L. Donaghay, and J. M. Sullivan, "Cryptic blooms: Are thin layers the missing connection?" *Estuaries and Coasts: J CERF*, vol. 31, pp. 396–401, 2008.

[9] J. J. Cullen, "Subsurface chlorophyll maximum layers: Enduring enigma or mystery solved?" *Annual Review of Marine Science*, vol. 7, pp. 207–239, 2015.

[10] Y. Zhang, R. S. McEwen, J. P. Ryan, and J. G. Bellingham, "Design and tests of an adaptive triggering method for capturing peak samples in a thin phytoplankton layer by an autonomous underwater vehicle," *IEEE Journal of Oceanic Engineering*, vol. 35, no. 4, pp. 785–796, October 2010.

[11] J. P. Ryan, R. M. Kudela, J. M. Birch, M. Blum, H. A. Bowers, F. P. Chavez, G. J. Doucette, K. Hayashi, R. Marin III, C. M. Mikulski, J. T. Pennington, C. A. Scholin, G. J. Smith, A. Woods, and Y. Zhang, "Causality of an extreme harmful algal bloom in Monterey Bay, California, during the 2014–2016 northeast Pacific warm anomaly," *Geophysical Research Letters*, vol. 44, pp. 1–9, 2017.

[12] Y. Zhang, B. Kieft, B. Hobson, J. Ryan, B. Barone, C. Preston, B. Roman, B.-Y. Raanan, R. Marin III, T. O'Reilly, C. Rueda, D. Pargett, K. Yamahara, S. Poulos, A. Romano, G. Foreman, H. Ramm, S. Wilson, E. DeLong, D. Karl, J. Birch, J. Bellingham, and C. Scholin, "Autonomous tracking and sampling of the deep chlorophyll maximum layer in an open-ocean eddy by a long range autonomous underwater vehicle," *IEEE Journal of Oceanic Engineering*, vol. 45, no. 4, pp. 1308–1321, 2020.

[13] B. Hobson, J. G. Bellingham, B. Kieft, R. McEwen, M. Godin, and Y. Zhang, "Tethys-class long range AUVs - extending the endurance of propeller-driven cruising AUVs from days to weeks," *Proc. IEEE AUV'2012*, pp. 1–8, Southampton, U.K., September 2012.

[14] S. Petillo, A. Balasuriya, and H. Schmidt, "Autonomous adaptive environmental assessment and feature tracking via autonomous underwater vehicles," *Proc. IEEE Oceans'10*, pp. 1–9, Sydney, Australia, May 2010.

[15] N. Cruz and A. C. Matos, "Reactive AUV motion for thermocline tracking," *Proc. IEEE Oceans'10*, pp. 1–6, Sydney, Australia, May 2010.

[16] Y. Zhang, J. G. Bellingham, M. A. Godin, and J. P. Ryan, "Using an autonomous underwater vehicle to track the thermocline based on peak-gradient detection," *IEEE Journal of Oceanic Engineering*, vol. 37, no. 3, pp. 544–553, July 2012.

[17] T. B. von See, J. Greinert, and T. Meurer, "Detection and tracking of ocean layers using an AUV with UKF based extremum seeking control in the Baltic Sea," *Scientific Reports*, p. 20629, 2024.

[18] Y. Zhang, B. W. Hobson, B. Kieft, M. A. Godin, T. Ravens, and M. Ulmgren, "Adaptive zigzag mapping of a patchy field by a long-range autonomous underwater vehicle," *IEEE Journal of Oceanic Engineering*, vol. 49, no. 2, pp. 403–415, 2024.

[19] J. G. Bellingham, Y. Zhang, J. E. Kerwin, J. Erikson, B. Hobson, B. Kieft, M. Godin, R. McEwen, T. Hoover, J. Paul,

A. Hamilton, J. Franklin, and A. Banka, “Efficient propulsion for the Tethys long-range autonomous underwater vehicle,” *Proceedings of IEEE AUV’2010*, pp. 1–6, Monterey, CA, September 2010.

[20] J. G. Bellingham and T. R. Consi, “State configured layered control,” in *Proc. IARP 1st Workshop on Mobile Robots for Subsea Environments*, Monterey, CA, October 1990, pp. 75–80.

[21] E. C. Orenstein, D. Ratelle, C. Briseño-Avena, M. L. Carter, P. J. S. Franks, J. S. Jaffe, and P. L. D. Roberts, “The scripps plankton camera system: A framework and platform for in situ microscopy,” *Limnology and Oceanography: Methods*, vol. 18, pp. 681–695, 2020.

[22] A.-S. Heiskanen and A. Keck, “Distribution and sinking rates of phytoplankton, detritus, and particulate biogenic silica in the Laptev Sea and Lena River (Arctic Siberia),” *Marine Chemistry*, vol. 53, pp. 229–245, 1996.

[23] C. A. Durkin, K. O. Buesseler, I. Cetinic, M. Estapa, R. P. Kelley, and M. Omand, “A visual tour of carbon export by sinking particles,” *Global Biogeochemical Cycles*, vol. 35, no. 10, pp. 1–17, 2021.

[24] S. J. Kramer, E. L. Jones, M. L. Estapa, N. L. Paul, T. A. Rynearson, A. E. Santoro, S. Sudek, and C. A. Durkin, “Sinking particles exporting diatoms and Hacrobia predict the magnitude of oceanic POC flux,” *The ISME Journal*, vol. 19, no. 1, p. wraf105, 2025.